Impact of Large Scale Wind Power with DFIG on Small Signal Stability of the System

Ankit Kumar Gupta[#], Alok Kumar Singh[*], Krishan Gopal Sharma[#]
[#]*M.Tech Scholar,Jaipur Institute of Technology-Group of Institution, Jaipur,Rajasthan, India*
[*]*Associate Professor, Dept. of Electrical Engineering, JIT-Group of Institution, Jaipur, Rajasthan, India*
[*]*Associate Professor & Head, Dept. of Electrical Engineering, Govt. Engg. college, Ajmer,Rajasthan, India*

Abstract

Future energy demand and increasing carbon emission requires an alternative source of energy. In recent few years, Use of DFIG based wind farm increased tremendously, thus effect of wind penetration on small signal stability of existing multi machine system need to be analysed. In This paper effect of penetration of wind turbine with DFIG on stability performance of the IEEE 9 bus and 39 bus system has been investigated using DIgSILENT power factory. It was observed that system with large number of buses is more stable with DFIG penetration then a small system.

Keywords - *DFIG, Energy, Penetration, Stability, Wind Turbine,*

I. INTRODUCTION

Nowadays with the increasing living standard the demand for electricity is also increasing. Due to fast depletion of fossil fuel and concern related to environment safety and meet future energy requirements all countries focus is increasing on renewable energy sources. Amongst all the renewable energy sources, solar and wind are the most popular energy source due to clean energy generation, zero fuel cost and renewable nature[1-4].

Nowadays these sources are not limited up to isolated system but also these are integrated to large power system with semiconductor power electronics device i.e. Converters and controllers[5]Among all the renewable energy technologies wind power is the most suitable because of its high efficiency in comparison with the other renewable energy sources like tidal, solar. In India, power generation by wind turbines was also increased in last few years. As per global status report, India ranked at 4th position among all the countries in the world in aspects of installed wind capacity till the end of 2015. By the end of 2002 the installed capacity of wind in India was 1.7GW which was increased to 7.1GW till the end of 2006-07, which have been further increased to 17.4GW with an increment of 10.3GW up to 2011-12. In 2016-17 it increased to 30.3GW (which is more than the target of 28.3GW) with an increment of 13.3 GW. Next target is to achieve 60GW of wind energy generation till 2021-22. Two categories of wind turbine generators (WTGs) are available: fixed and variable speed. In early years, Squirrel cage induction generators(SCIG) which is a fixed speed WTG were used but Nowadays doubly fed induction generators (DFIG) are prominent because these are variable speed WTGs[6]. DFIG equipped wind turbine is presently the most widely used because it is capable of controlling reactive power, have high efficiency, and the fact that the power electronic converter rating is about 20%-30% of the total machine power is needed. With small integration of wind power its impact is minimal but with the increased level of wind power penetration on the existing large power system may affect the dynamic performance of the system. Thus, it is essential for power system engineers to investigate and understand the effects of wind power penetrations on existing power system. Especially, for the small signal stability of power system [4]

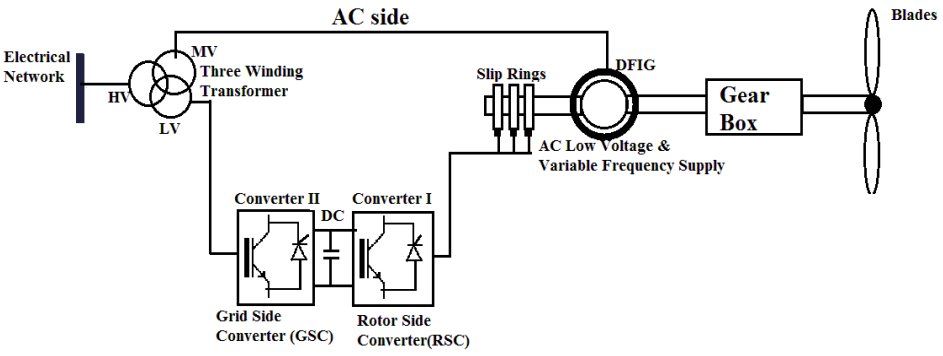

FIG.1: DFIG

II. MODELLING OF WIND ENERGY SYSTEM WITH DFIG

A. Electrical dynamics

Schematic diagram of DFIG connected with electrical network is shown in fig.1.[7]DFIG type of wind generators can operate in two modes, first one is super-synchronous mode and second one is sub-synchronous mode with ±30% of synchronous speed.

Rotor circuit is controlled by voltage source converter connected through slip rings and stator is directly connected to the grid. Back to back VSCs are included in the rotor circuit. Only 30% of the rated electric power is handled by these power electronic converter converters.

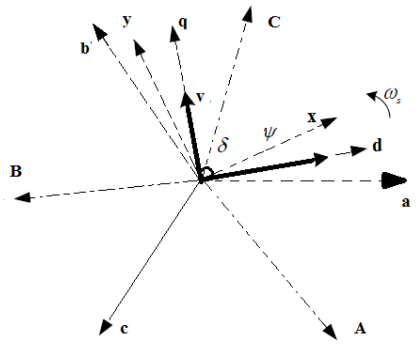

Fig.2 d-q reference frame

In synchronous rotating reference frame shown in fig.2[8] the basic equation of asynchronous machine can be written as follow.

Equations for Stator

$$v_{ds} = -R_s i_{ds} - \omega_s \varphi_{qr} + \frac{1}{\omega_{base}} \frac{d}{dt} \varphi_{ds} \quad (1)$$

$$v_{qs} = -R_s i_{qs} + \omega_s \varphi_{ds} + \frac{1}{\omega_{base}} \frac{d}{dt} \varphi_{qs} \quad (2)$$

Equations for rotor

$$v_{dr} = -R_r i_{dr} - s\omega_s \varphi_{qr} + \frac{1}{\omega_{base}} \frac{d}{dt} \varphi_{dr} \quad (3)$$

$$v_{qr} = -R_r i_{qr} + s\omega_s \varphi_{dr} + \frac{1}{\omega_{base}} \frac{d}{dt} \varphi_{qr} \quad (4)$$

In d-q reference frame rotating with synchronous speed ω_s A, B, and C indicates rotor phase winding axes, a, b and c represents stator phase winding axes.

In the equation, Subscript r and s represents rotor and stator and Q and d represents quadrature and direct axis. stator voltage for direct and quadrature axis are represented by (v_{ds}, v_{qs}),voltage for the direct and quadrature axis of rotor is (v_{dr}, v_{qr}), the stator resistance, rotor resistance, stator reactance, rotor reactance, mutual reactance, slip, synchronous. speed, rotor speed, base frequency and electromechanical torque are represented by R_s, R_r, X_s, X_r, X_m, s, ω_s, ω_r, ω_{base}, T_{em} respectively.

The related flux equation in d-q frame are as follow:

Equations for rotor:

$$\varphi_{dr} = -(X_r i_{dr} + X_m i_{ds}) \quad (5)$$

$$\varphi_{qr} = -(X_r i_{qr} + X_m i_{qs}) \quad (6)$$

Equations for Stator

$$\varphi_{ds} = -(X_s i_{ds} + X_m i_{dr}) \quad (7)$$

$$\varphi_{qs} = -(X_s i_{qs} + X_m i_{qr}) \quad (8)$$

B. Power dynamics

Power injected to the grid is mainly depends on converter operating modes. Hence the converter Power on RSC and GSC are represented by following equations:

$$P_g = v_{dg} i_{dg} + v_{qg} i_{qg} \quad (9)$$

$$Q_g = v_{qg} i_{dg} - v_{dg} i_{qg} \quad (10)$$

$$P_r = v_{dr} i_{dr} + v_{qr} i_{qr} \quad (11)$$

$$Q_r = v_{qr} i_{dr} - v_{dr} i_{qr} \quad (12)$$

C. Mechanical Model

Drive train model of wind turbine is shown in Fig.3. Model is divide in two parts low speed and high-speed model. In the blade side model which is low speed model J_b, D_b and ω_b represents inertia constant, damping constant for blade side and speed of blades. Where in generator side model J_g, Dg and ω_r represents inertia constant, damping constant for generator side and speed of rotor:

Equations for the drive train model are as follow:

$$\frac{d\theta_b}{dt} = \omega_b \quad (13)$$

$$\frac{d\theta_r}{dt} = \omega_r \quad (14)$$

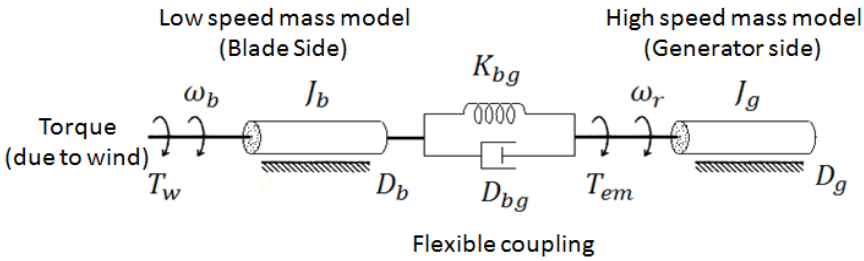

Fig.3 Drive Trin Model of DFIG

$$\frac{d\omega_r}{dt} = \frac{1}{J_g}\left(K_{bg}(\theta_b - \theta_r) + D_{bg}(\omega_b - \omega_r) - D_g\omega_r - T_{em}\right) \quad (15)$$

$$\frac{d\omega_b}{dt} = \frac{1}{J_b}\left(T_w - D_b\omega_b - D_{bg}(\omega_b - \omega_r) - K_{bg}(\theta_b - \theta_r)\right) \quad (16)$$

Θ_b are Θ_r the angular displacements, D_{bg} and K_{bg} are damping constant and stiffness of the flexible coupling respectively.

T_w represents wind torque which is as follow:

$$T_w = \frac{P_w}{\omega_m} \quad (17)$$

Where mechanical POWER extracted from the wind is P_w which is expressed as

$$P_w = \frac{\rho}{2} C_p(\lambda, \theta_p) A_r v_w^3 \quad (14)$$

where ρ, v_w, Θ_p, C_p, A_r and k is the air density, speed of wind, pitch angle, Power coefficient area swept by the rotor and blade tip speed ratio respectively[9].

T_w represents wind torque which is as follow:

$$T_w = \frac{P_w}{\omega_m} \quad (18)$$

Where mechanical power extracted from the wind is P_w which is expressed as

$$P_w = \frac{\rho}{2} C_p(\lambda, \theta_p) A_r v_w^3 \quad (19)$$

where ρ, v_w, Θ_p, C_p,A_r and k is the air density, speed of wind , pitch angle, Power coefficient area swept by the rotor and blade tip speed ratio respectively.

D. Converter Dynamics

The DFIG system consist of two converters connected back to back as shown in fig.1.one is rotor side converter(RSC) and another is grid side converter(GSC). RSC acts as a controlled voltage and GSC acts as a controlled current source. The rotor side converter can be used as torque controller, speed controller and active power controller to regulate the output power of DFIG. The rotor currents are also used to control the reactive power production in DFIG.

Let, V_{DC} be the DC link voltage, m_d and m_q be the modulation depth setup by RSC for direct and quadrature components, respectively.[10] So, the rotor voltage components for voltage and current can be written as

$$v_{rd} = m_d \frac{\sqrt{3}v_{DC}}{2\sqrt{2}} \quad (20)$$

$$v_{rq} = m_q \frac{\sqrt{3}v_{DC}}{2\sqrt{2}} \quad (21)$$

Total active power and reactive power or the total active power and the stator voltage are the quantities that is to be controlled. Through the Rotor only a small part of the total active power is exchanged. Equation for the stator active power can be written as

$$P_S = -\frac{x_m}{x_s}(v_{sd}i_{dr} + v_{sq}i_{qr}) \quad (22)$$

Grid side converter is used to control the voltage of the DC link, present between the rotor side converter and grid side converter. And it is also allowed to generate and absorb reactive power for voltage support requirements to control the reactive power between the rotor and the grid GSC is controlled. Total reactive power can be controlled by controlling the stator reactive power. The stator reactive power can be expressed as

$$Q_S = \frac{x_m}{x_s}(v_{sd}i_{qr} - v_{sq}i_{dr}) - \frac{1}{x_S}|\bar{v_s}|^2 \quad (22)$$

III.STEADY STATE ANALYSIS

Stability of a system is defined as the ability to regain synchronism after being subjected to disturbances. There are two types mainly voltage stability and rotor angle stability.[11, 12] Oscillation with a couple of hertz frequency, mostly occurs in the power system are mainly focused under rotor angle stability. These oscillation with frequency about 0-2hz define the small signal oscillation and the small signal stability of the system. Due to the variation in the system load and power generation these oscillations occur all the time.

To analyse the small signal stability of a large system Modal analysis can be used. A power system with large no. of buses can be linearized by a set of n linear differential equations with first order. known as state space model[12].

A. Eigen Value Analysis

One of the powerful tool to analyze the small signal stability of a system is computing and analyzing eigen values of the system. For eigen values computation at first, we have to linearize the system in a set of n first order Differential algebraic equations(DAE), which is known as ABCD model. Thus, from the state space model eigen values can be computed using a state matrix[12].

In small signal analysis, the DAEs describing the complete power system are linearized in linear model using Taylor series is as (23) -(25). Where x represent the state variable and y denotes the control input and system output respectively represent the column vector of DE and column vector of algebraic equation is represented by g. Here, Δ denotes the small deviation.

$$\frac{d}{dt}\mathbf{x} = \mathbf{f}(\mathbf{x}, \mathbf{u}) \quad (23)$$

$$\mathbf{y} = \mathbf{g}(\mathbf{x}, \mathbf{u}) \quad (24)$$

$$x = \begin{bmatrix} x_1 \\ x_2 \\ x_3 \\ \vdots \\ x_n \end{bmatrix} \quad u = \begin{bmatrix} u_1 \\ u_2 \\ u_3 \\ \vdots \\ u_n \end{bmatrix} \quad y = \begin{bmatrix} y_1 \\ y_2 \\ y \\ \vdots \\ y \end{bmatrix} \quad f = \begin{bmatrix} f \\ f_2 \\ f_3 \\ \vdots \\ f_n \end{bmatrix} \quad g = \begin{bmatrix} g_1 \\ g_2 \\ g_3 \\ \vdots \\ g_n \end{bmatrix} \tag{25}$$

Equation 23,24, and 25 can be written in the following form:

$$\Delta\dot{x} = \left[\frac{\partial f}{\partial x}\right]_0 \Delta x + \left[\frac{\partial f}{\partial u}\right]_0 \Delta u \tag{26}$$

$$0 = \left[\frac{\partial g}{\partial x}\right]_0 \Delta x + \left[\frac{\partial g}{\partial u}\right]_0 \Delta u \tag{27}$$

$$\Delta\dot{x} = A\Delta x + B\Delta u \tag{28}$$

$$\Delta y = C\Delta x + D\Delta u \tag{29}$$

where A, B, C, D, are the Jacobian matrices of dimension N*N, which are defined as below:

$$A = \left.\frac{\partial f(x,y)}{\partial x}\right|_{x_0,y_0}; B = \left.\frac{\partial f(x,y)}{\partial y}\right|_{x_0,y_0}$$

$$C = \left.\frac{\partial g(x,y)}{\partial x}\right|_{x_0,y_0}; D = \left.\frac{\partial g(x,y)}{\partial y}\right|_{x_0,y_0} \tag{30}$$

Here A is the system matrix. Small signal stability analysis of the system can be done by eigen values ($\lambda = \sigma \pm \omega$) of system matrix A, where σ is the real part and ω is imaginary part of the eigen value represents the damping and frequency of oscillations respectively. Negative real part $(-\sigma)$ means the system is damped and stable. Where positive real part $(+\sigma)$ means that the system oscillation are with increasing amplitude which will leads system towards the unstable system.[13].

The Damping ratio of the system describes the decay rate of the amplitude of oscillations, the Damping frequency of oscillations (in Hz) and the time constant is expressed as (31) -(33)

$$\zeta = -\sigma/\sqrt{\sigma^2 + \omega^2} \tag{31}$$

$$f = \frac{\omega}{2\pi} \tag{32}$$

$$\tau = \frac{1}{|\sigma|} \tag{33}$$

Sometimes participation factor is also used in Small signal stability analysis for the measurement of relative participation in that particular mode. For n state variables, in i_{th} mode participation factor(P_i) is defined as:

$$P_{ki} = \frac{|\psi_{ik}||\phi_{ki}|}{\sum_{k=1}^{n}|\psi_{ik}||\phi_{ki}|} \tag{34}$$

Where ψ_{ik} represents K th element of i th mode left eigen vector and ϕ_{ki} denotes i th element of k th mode right eigen vector. A lower P_{ki} indicates that eigen value λ_i for i th mode is less sensitive to the k th state variable x_k and larger P_{ki} indicates that λ_i for i th mode is more sensitive to the Kth state variable x_k.

IV. TEST SYSTEM AND APPROACH

For study and simulation two different systems were taken. At first the study of IEEE 3 machine 9 bus system has been done with and without DFIG. Then IEEE 10 machine 39 bus system have been studied.

Case I: IEEE 3 machine 9 bus system have been used to analyse. DFIG is connected one by one at different bus at which synchronous generator is connected.

Case II: IEEE 39 bus New England System have been used for case study. DFIG is connected one by one at each bus of synchronous generator by replacing synchronous generators.one by one all 10 generators are replaced by DFIG and the eigenvalues have been computed.

Compete simulation have been performed using DIgSILENT PowerFactory Simulator.

V. RESULTS AND ANALYSIS

Case I: Grid summary for IEEE 3 machine 9bus system is shown below in Table I

Table I Load Flow Summary IEEE 9 Bus system

Generation	6140.81 MW	1250.37 MVAr
Load	6097.10 MW	1408.9 MVAr
Grid losses	43.71 MW	-158.53 MVAr
Installed capacity		14535.00 MW
Spinning reserve		8394.19 MVAr
Power factor		0.97 Lagging

One by one DFIG was connected at three different buses at which synchronous generator is connected by replacing the synchronous generator. Eigen values have been calculated by QR/QZ method on DIgSILENT PowerFactory simulator tool[14]. The eigen values for all three location are calculated and the complex eigen value with least real par (λ_{min}) near to imaginary axis are shown in Table II

Table II Eiegn Values for IEEE 3 Machine 9 Bus System

Bus No. at which DFIG connected	Eigen Value(λ_{min})	
	Real part	Imaginary Part
Without DFIG	-0.6288	±j8.6851
Bus 1	-0.7435	±j8.8458
Bus 2	-0.5936	±j9.1278
Bus 3	-0.6301	±j2.4764

Minimum eigenvalue (λ_{min}) without DFIG is 0.6288±j8.6851. σ_{min} represents the real part of minimum eigen value $\lambda_{min.}$ From the Table II. It can be seen that when DFIG replaces synchronous generator at bus 2 eigen values is shifted towards the right. As we know that movement of real part towards right means the system stability is decreasing and vice versa. Also, it can be seen that when Synchronous generator is replaced by DFIG at bus 1 the improvement of σ_{min} is highest means shifting eigen values towards the left side which leads to improvement in system stability. Thus, bus 1 is the suitable location for DFIG.

Case II: IEEEE 39 bus system have been used for study. Grid summary for IEEE 39 bus is shown in Table III.

Table III Load Flow Summary IEEE 39 Bus System (New England System)

Load Flow summary 9 Bus System		
Generation	6140.81 MW	1250.37 MVAr
Load	6097.10 MW	1408.9 MVAr
Grid Losses	43.71MW	-158.53 MVAr
Installed Capacity		14535.00 MW
Spinning Reserve		8394.19 MVAr
Power Factor		0.97 Lagging

Analysis approach is similar as case I. DFIG is connected at same bus at which synchronous generator is connected. Complex eigen values with minimum real part have been calculated using Lanczo's/ Arnoldi's method. Eigen value for all 10 different scenarios have been listed in Table III.

Table IV. Eiegn Values for IEEE 3 Machine 9 Bus System

Bus No. at which DFIG connected	Eigen Value (λ_{min})	
	Real part	Imaginary Part
Without DFIG	-0.12524247	±j0.430038734
Bus 30	-0.151361	±j0.521454107
Bus 31	-0.13159529	±j0.459232551
Bus 32	-0.1256043	±j0.44118654
Bus 33	-0.12560279	±j0.458345069
Bus 34	-0.12675018	±j0.449177865
Bus 35	-0.12529636	±j0.459423962
Bus 36	-0.12646815	±j0.45216573
Bus 37	-0.20023535	±j0.470844042
Bus 38	-0.12578821	±j0.459898094
Bus 39	-0.12530811	±j0.440076499

The σ_{min} without DFIG is -0.12524±j0.430038734. after relacing synchronous generator one by one with DFIG wind farm of same capacity different eigen values have been obtained. From Table II it can be seen that effect of connecting DFIG is maximum when it was connected at bus 37. Maximum improvement in σ_{min} is obtained when DFIG was connected at bus 37. Fro table II it can be seen that the σ_{min} is shifting towards the left side of plane for all 10 buses which results in improving system stability.

VI. CONCLUSION

Eigen value analysis have been performe for muli machine system with and without penetration of wind power with DFIG. Minimum eigen value(λ_{min}) has been find out for each bus for both IEEE9 bus and 39 Bus system. And effect of DFIG wind farm was analysed on the small signal stability pwerformnce of the system. It was observed that penetration of DFIG wind farm in 9 bus system make system unstable when DFIG replace SG at bus 2, also the system become s more stable when DFIG is connected at bus 1 or 3. Similiarly,for 39 bus system it was observed that sytem becomes more stable when DFIG is connected to the system. Best location for the DFIG connection is bus 37 because of the maximimum improvement in the minimum eigen value.

ACKNOWLEDGMENT

I wish to express my deep sense of gratitude towards my guide Mr. Alok Singh (Assistant Professor, Department of Electrical Engineering, Jaipur Institute of Technology, Jaipur) and Dr. Krishan Gopal Sharma (Head & Associate Professor, Department of Electrical Engineering, Govt. Engineering College, Ajmer) for his guidance and encouraging support which were invaluable for the completion of this work.

My Sincere thanks are due to Dr. Ravi Goyal (Principal, JIT, Jaipur) for his valuable inputs in completion of this work.

REFERENCES

[1] C. Sheng, J. Zeng, W. Chu, and Y. Zeng, "Study on Modeling Simulation and Identification of Wind Generator Based on DIgSILENT," in Power and Energy Engineering Conference (APPEEC), 2012 Asia-Pacific, 2012, pp. 1-5: IEEE.

[2] H. Iswadi, D. J. Morrow, and R. J. Best, "Small signal stability performance of power system during high penetration of wind generation," in Power Engineering Conference (UPEC), 2014 49th International Universities, 2014, pp. 1-6: IEEE.

[3] T. Ackermann, Wind power in power systems. John Wiley & Sons, 2005.

[4] L. Wang, Y.-F. Lin, and S.-C. Ke, "Stability analysis of an offshore wind farm connected to Taiwan power system using DIgSILENT," in OCEANS 2014-TAIPEI, 2014, pp. 1-5: IEEE.
[5] R. Krishan, A. Verma, and B. Prasad, "Small signal stability analysis of grid connected distributed PV and wind energy system," in Power India International Conference (PIICON), 2014 6th IEEE, 2014, pp. 1-6: IEEE.
[6] D. Gautam, V. Vittal, and T. Harbour, "Impact of increased penetration of DFIG-based wind turbine generators on transient and small signal stability of power systems," IEEE Transactions on Power Systems, vol. 24, no. 3, pp. 1426-1434, 2009.
[7] B. Mehta, P. Bhatt, and V. Pandya, "Small signal stability analysis of power systems with DFIG based wind power penetration," International Journal of Electrical Power & Energy Systems, vol. 58, pp. 64-74, 2014.
[8] C. Wang, L. Shi, L. Wang, and Y. Ni, "Small signal stability analysis considering grid-connected wind farms of DFIG type," in Power and Energy Society General Meeting-Conversion and Delivery of Electrical Energy in the 21st Century, 2008 IEEE, 2008, pp. 1-6: IEEE.
[9] D. R. Chandra et al., "Impact of SCIG, DFIG wind power plant on IEEE 14 bus system with small signal stability assessment," in Power Systems Conference (NPSC), 2014 Eighteenth National, 2014, pp. 1-6: IEEE.
[10] C. Hamon, K. Elkington, and M. Ghandhari, "Doubly-fed induction generator modeling and control in DigSilent PowerFactory," in Power System Technology (POWERCON), 2010 International Conference on, 2010, pp. 1-7: IEEE.
[11] B. K. Kumar, "Power system stability and control," Department of Electrical Engineering, Indian Institute of Technology Madras, Chennai, India, 2004.
[12] P. Kundur, N. J. Balu, and M. G. Lauby, Power system stability and control. McGraw-hill New York, 1994.
[13] S. Kong, R. Bansal, and Z. Dong, "Comparative small-signal stability analyses of PMSG-, DFIG-and SCIG-based wind farms," International Journal of Ambient Energy, vol. 33, no. 2, pp. 87-97, 2012.
[14] D. PowerFactory, "Digsilent powerfactory 15 user manual," ed: August, 2013.